ISSN 0022-4766, Journal of Structural Chemistry, 2020, Vol. 61, No. 4, pp. 659-667. © Pleiades Publishing, Ltd., 2020.
Russian Text © The Author(s), 2020, published in Zhurnal Strukturnoi Khimii, 2020, Vol. 61, No. 4, pp. 691-700.

COMPUTER STUDY OF SILICENE APPLICABILITY IN ELECTROCHEMICAL DEVICES

A. E. Galashev[1,2]* and K. A. Ivanichkina[1]

Novel anode materials made of silicene on metal substrates are studied by molecular dynamics. Ni(111) and Cu(111) substrates are most preferable in terms of higher anode's occupancy and mechanical strength. The highest crystallinity degree is exhibited by the lithium packing in the silicene channel on the Ag(111) substrate. The lowest local normal stresses appear in the walls of the channel on the Al(111) substrate. The voltage profile is built as a function of concentration of Li adsorbed on free-standing bilayer silicene.

DOI: 10.1134/S0022476620040204

Keywords: lithium, molecular dynamics, self-diffusion, silicene, structure.

INTRODUCTION

No natural layered silicon with a structure similar to that of graphite has been found so far. However, thin silicon film consisting of one or several atomic layers were prepared by depositing Si atoms onto certain metal surfaces [1-4]. For example, two-dimensional silicon monolayers formed by hexagonal cells could be obtained using hexagonal symmetry of the Ag(111) surface [5]. Such films are referred to as silicene. The existence of silicene is proved by the fact that some of its specific electronic properties are also exhibited by graphene: e.g., it was discovered that silicene demonstrates linear dispersion at points K, K′ of the Brillouin zone [6]. As is known, silicon has a high theoretical specific capacity (4200 mAh/g) and can be viewed as the primary candidate for anode materials in lithium-ion batteries (LIBs) [7]. However, crystalline silicon undergoes strong volume changes during cycling and is therefore fairly rapidly destroyed. Silicene lacks this disadvantage and seems to be a promising material for LIB anodes. Silicene prepared by epitaxial growth can not be separated from the substrate; however, its electronic properties are greatly affected by metal substrates: usually, silicene on such substrates acquires metallic properties. Enhanced electronic conductivity favors its use as the anode material.

When entering crystalline silicon, Li^+ ions diffuse along a tortuous path corresponding to the smallest radius of Si valence orbital [8]. In other words, the diffusion of Li^+ into crystalline Si is anisotropic and follows highly tortuous diffusion pathways so that it quite rapidly captures an electron and becomes an atom. Starting from this point, it is an atom rather than an ion that diffuses in the silicon. In graphite, the lifetime of the Li^+ ion is much larger, which is, in particular, due to the fact that the ionization potential of the C atom is almost 1.4 times higher than that of the Si atom. The radius of the C atom is 1.8 times smaller than that of the Si atom. As a result, the distance between two nuclei is smaller in carbon than in silicon. The overlap between *p* orbitals of two carbon atoms is more effective due to smaller internuclear distances. Therefore, the overall

[1]Institute of High Temperature Electrochemistry, Ural Branch, Russian Academy of Sciences, Ekaterinburg, Russia; *galashev@ihte.uran.ru. [2]Yeltsin Ural Federal University, Ekaterinburg, Russia. Original article submitted September 3, 2019; revised October 3, 2019; accepted October 15, 2019.

electronic structure of solid carbon materials is considerably more stable than that of silicon materials. The electron transfer to the Li^+ ion is more difficult in carbon materials.

When a lithium-ion battery is being charged, lithium ions pass through the electrolyte, reach the silicon electrode, and join with electrons to form lithium atoms [9]. This process occurs at the boundary between the electrolyte and the Li_xSi surface. This is facilitated by a the fact that the electron conductivity of Li_xSi compounds is higher than that of silicon. The diffusion throughout the silicon volume is due to Li atoms rather that Li ions. At the same time, diffusion of lithium ions in graphite was proved experimentally [10].

In this work, a channel formed by two silicon sheets is considered as an anode element. The channel was placed on different metal substrates (Ag, Al, Ni, Cu). The processes Li^+ ion intercalation and deintercalation for the considered anode element were studied by molecular dynamics (MD). In addition to the effect of the substrate material on the course of this processes, we also considered the effect of defects on the strength of the channel walls and its occupancy by lithium.

The purpose of this work is to consider the use of bilayer defective silicene located on different metal substrates as the anode material for lithium-ion batteries.

COMPUTANIONAL MODEL

Silicene sheets with a flower-like structure [11] were arranged horizontally one above the other. The rhombic unit cell of silicene contained 18 atoms, 6 of which were raised above the main plane [12]. The gap h_g between the sheets was empirically chosen to be 0.75 nm to let lithium atoms diffuse freely through the channel [13]. The channel formed by silicene sheets was placed on some metal (Ag, Al, Ni, Cu) substrate directed by its (111) face to the channel. The channel had no solid sidewalls but was surrounded by an artificial force barrier preventing the atoms from exiting through side and back surfaces [14]. Li^+ ions were periodically introduced into the channel through the entry gate (front surface) every 10 ps. They were introduced either in pairs or singly and were "drawn" into the channel due to the action of a 10^3 V/m electric field. 10 ps later, the introduced Li^+ ion was transformed into a lithium atom [14] which did not "feel" the electric field. In other words, intercalation was simulated by silicene ions entering the silicene channel from a solid electrolyte, as it is shown in Fig. 1 for the case of a nickel substrate. The channel walls were represented by sheets of perfect or defective silicene. The sheet size was 4.8×4.1 nm. Nine defects were located almost uniformly on each silicene sheet. The defects were mono-, bi-, tri-, and hexavacancies.

The procedure of ion filling was carried out until the channel was completely filled with lithium. After the filling limit was reached, the ions could no longer enter the channel and moved beyond its boundaries. The deintercalation was started by reversing the direction of electric field vector while increasing the field strength up to 10^5 V/m. The ion or the pair of ions which were the last to enter the channel were the first to begin the deintercalation process, and then their predecessors

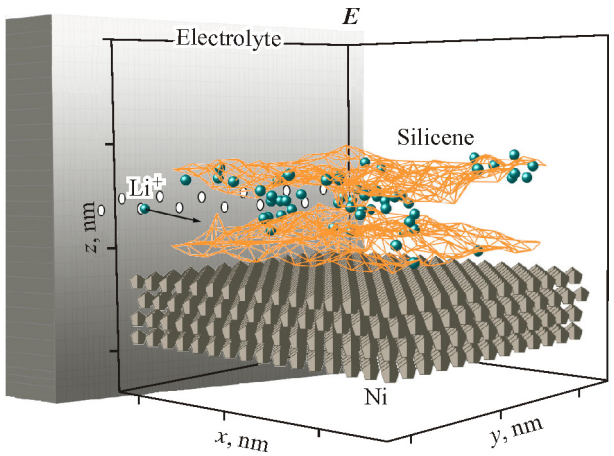

Fig. 1. Channel formed by perfect silicene sheets on a nickel substrate after lithium intercalation.

during the intercalation stage were transformed into ions. After that, they were removed from the channel under the action of electric field. This process continued until the channel was empty.

The interaction between Si atoms on the same silicene sheet was simulated the Tersoff potential [15]. The interaction between metal atoms in the substrate was described by the embedded-atom potential [16]. Cross-interactions, including those between Si atoms from different silicene sheets, were simulated by the Morse potential [17-19]. If two ions were simultaneously present in the channel, the Coulomb interaction between them was calculated in addition to the interatomic interaction.

The self-diffusion coefficient of lithium atoms in the silicene channel was determined from the following expression:

$$D = \lim_{t \to 0} \frac{1}{2\Gamma t} \langle [\Delta \mathbf{r}(t)^2] \rangle, \quad (1)$$

where Γ is the dimension of the space; $\langle [\Delta \mathbf{r}(t)]^2 \rangle$ is the mean square displacement of the atoms; symbol $\langle \ldots \rangle$ means that a quantity is averaged over time.

The stress distribution in silicene sheets was studied as follows. A silicene sheet was divided into surface elements elongated along "chair" or "zigzag" directions and having normals γ (x, y, z). The resultant force acting on each surface element was calculated in the course of intercalation (deintercalation). The resultant force included only those interactions between atoms i–j whose force vectors passed through the considered surface element [20]. In addition, the calculation of $\sigma_{\gamma\alpha}(l)$ took into account the direction α (x, y, z) of the velocities of atoms i and j:

$$\sigma_{\gamma\alpha}(l) = \left\langle \sum_i^n \frac{1}{\Omega} (m v_\gamma^i v_\alpha^i) \right\rangle + \frac{1}{S_l} \left\langle \sum_i^n \sum_{j \neq i}^{(u_i \leq u,\, u_j \geq u)} (f_{ij}^\alpha) \right\rangle. \quad (2)$$

The following designations were used in expression (2): n is the number of atoms on the element l; Ω is the volume per atom; v_α^i is the α projection of the velocity vector of atom i; S_l is the area of element l; m is the mass of the atom; f_{ij}^α is the α projection of the resultant force vector between atoms i and j passing through element l; u_i is the current coordinate of atom i (u in the upper bound of summation denotes the coordinate of the intersection point between the line passing through the centers of atoms i and j and element l).

The analysis of lithium packings in the channel was carried out by constructing Voronoi polyhedra (VPs). One main characteristic of this method of structural study is angular distribution of the nearest geometric neighbors determined by angle θ whose vertex coincides with the VP center and the sides pass through this vertex and the centers of two atoms which are the nearest neighbors.

Lithium interacts stronger with silicene than with graphene [21]; therefore, silicene can contain more lithium ions than graphene and is consequently expected to have a larger charge capacity. The maximum concentration of lithium adsorbed on silicene without breaking Si–Si bonds was determined using a separate molecular dynamics calculation. The calculation was carried out for bilayer silicene with a gap between the sheets equal to h_g = 0.75 nm and a packing represented by a 4×4 supercell containing 18 atoms [12, 22]. Each silicene sheet contained 54 atoms. The sheets were placed one above the other parallel to the xy plane; the size of each sheet was 1.90×2.25 nm taking into account the size of Si atoms. Silicene was placed in a rectangular "box" with impenetrable walls so that the distances between all outer Si atoms and the walls were approximately equal. Initially, the "box" was randomly filled with 300 Li atoms so that the minimal distance between Li and Si atoms or Li and Li atoms was at least 0.27 nm. Then a MD calculation was performed for 5 million time steps (one step Δt was 10^{-16} s). As a result, Li atoms filled the channel formed by silicene sheets and adsorbed on the outer walls of the channel. The Li atoms which were not connected to silicene directly or through other Li atoms were removed from the system. If some Si atoms moved away from the sheet farther than by 0.30 nm (the Si–Si bond length in silicene is 0.228 nm), silicene was interpreted to be destroyed under the action of adsorbed Li atoms. In such case, the MD calculation was repeated with the number of Li atoms being diminished by 5.The finally obtained non-destructive silicene configuration was used as the initial

geometry for DFT (density function theory) calculations. The concentration of lithium in the system preceding the one chosen for DFT calculations will be denoted by x_2.

The concentration dependence of electric potential was searched by performing DFT calculations [24] which were carried out with the SIESTA program [23] using appropriate pseudopotentials [25], the Perdew, Burke and Ernzerhof (PBE) generalized gradient approximation (GGA) [26], a plane wave basis set, and a kinetic energy cutoff of 200 Ry. The Brillouin zone was determined by *the Monkhorst–Pack method* using a 10×10×1 k-point set [27].

The system with non-destructive silicene obtained as a result of MD simulation was subjected to dynamic relaxation within the DFT model. Then a certain proportion of randomly chosen Li atoms (starting from the outer sides of bilayer silicene) was removed from the system to make it concentration equal to x_1, and dynamic relaxation was repeated. The resulting system corresponded to the state achieved due to partial deintercalation (current state with lithium concentration equal to x_1). The deintercalation process was divided into 10 parts, i.e. 10 values x_1 were calculated. The procedures of searching initial configurations of nondestructive silicene and the "intercalation/deintercalation" cycle were repeated three times with different random numbers corresponding to the numbers of lithium atoms.

According to [28], the dependence of the voltage generated by the silicene element on the concentration of intercalated lithium ions is

$$V(x) = \frac{-[E_{\mathrm{Li}x2\mathrm{Si}} - E_{\mathrm{Li}x1\mathrm{Si}} - (x_2 - x_1)E_{\mathrm{Li}}]}{(x_2 - x_1)e}, \quad (3)$$

where x_1, x_2 is the current concentration of lithium in silicene and its concentration at the initial stage of the filling of bilayer silicene; $E_{\mathrm{Li}x1\mathrm{Si}}$, $E_{\mathrm{Li}x2\mathrm{Si}}$ are the energies of the "silicene–lithium" system for lithium concentrations x_1 and x_2, respectively; E_{Li} is the total energy of bulk metal lithium; e is the elementary electric charge.

Parallel calculations were conducted using the standard LAMMPS software for MD simulations [29]. The software was supplemented by the fragments allowing one to calculate kinetic and mechanical properties of the system. The calculations were performed on the URAN hybrid computational cluster of IMM UB RAS with a peak performance of 216 Tflop/s and a 1864 CPU.

RESULTS AND DISCUSSION

In this study, not only best metal substrates for the channel were searched but also optimal sizes of silicene defects to achieve the highest occupancy of the channel by lithium. Fig. 2 shows the utmost occupancy of the silicene channel by

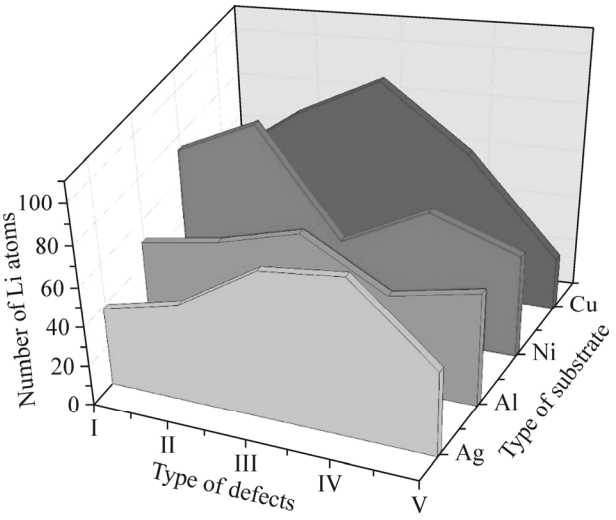

Fig. 2. The utmost number of Li atoms intercalated in the silicene channels on Ag, Al, Ni, and Cu substrates. Perfect silicene channel (I), channel walls with mono-, bi-, tri-, and hexavacancies, respectively (II-V).

lithium for the channels placed on various metal substrates. The substrate type was used as one parameter and the defect type was used as the other parameter. The defects were designated by Roman numerals. The highest occupancy was obtained for the channel with single vacancies on a Ni(111) substrate and for the channel with bivacancies on a Cu(111) substrate.

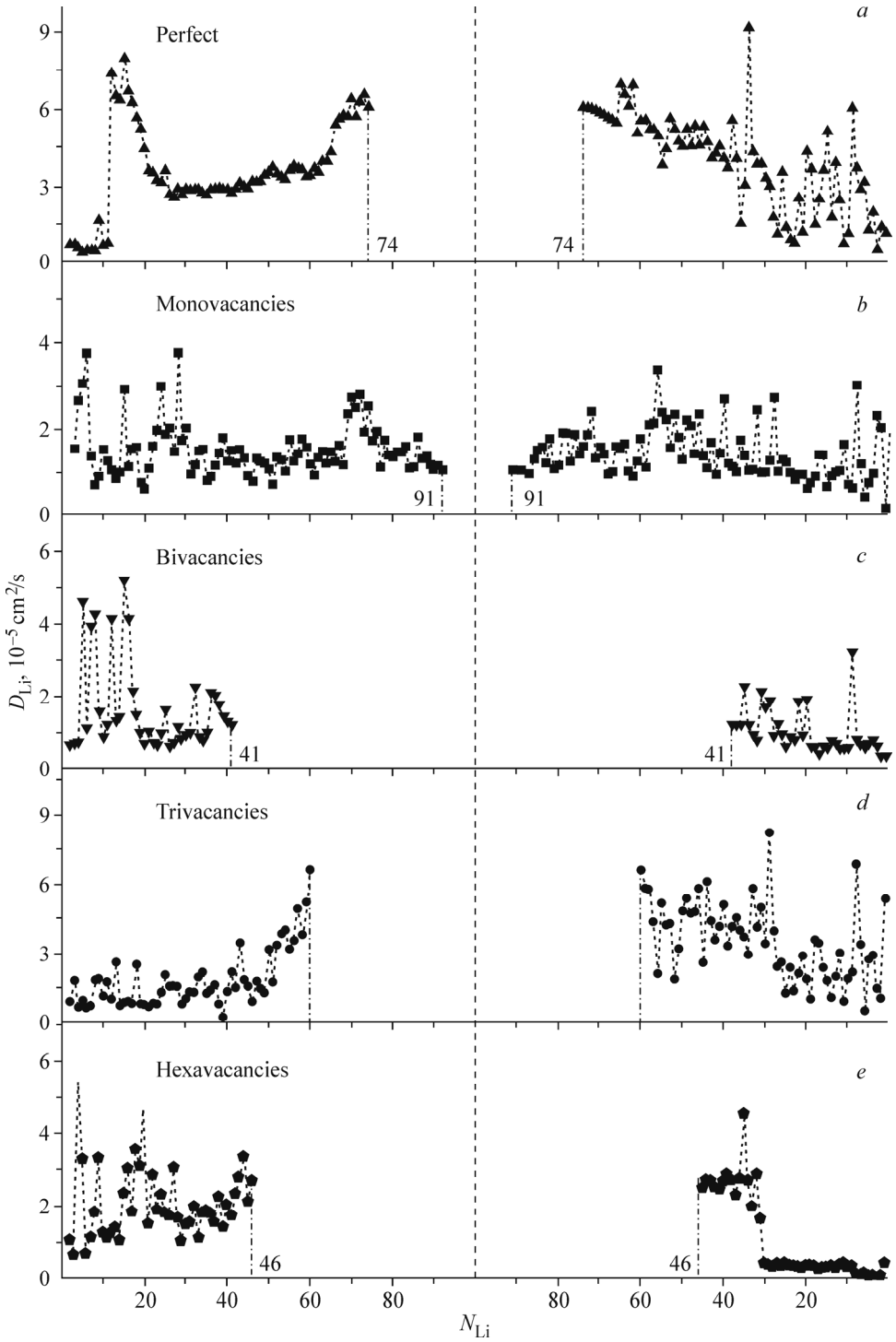

Fig. 3. Self-diffusion coefficient of lithium atoms in the course of intercalation (left) and deintercalation (right) in different silicene channels on the Ni(111) substrate: perfect silicene (*a*), silicene with monovacancies (*b*), bivacancies (*c*), trivacancies (*d*), and hexavacancies (*e*). The utmost number of lithium atoms in the channels is shown by the dashed line.

The self-diffusion coefficient D of lithium atoms in the channel is ~10^{-5} cm^2/s, which is quite a large value (Fig. 3). This is an encouraging result, since large D values should lead to high charge rates of the battery; moreover, this value is strongly fluctuating when viewed as a function of the number of lithium atoms in the channel. At the initial intercalation stage, fluctuations of D are larger since the process is yet unsteady. At the final deintercalation stage, the amplitude of fluctuations of D in the defective channels usually decreases due a lower number of collisions between lithium atoms. However, no such reduction in the amplitude of D fluctuations is observed in the channel with perfect silicene walls, which is explained by an increased number of collisions between lithium atoms and ions and the walls in the final deintercalation stage.

As the channel is filled with lithium, its walls get strained and may finally collapse. It is therefore important to know stress distribution along the channel in different directions. Fig. 4 shows the distribution of normal stresses (with respect to the channel walls) along the "chair" direction of atomic rows in the channel. The stresses in the silicene walls with monovacancies are shown for the channels placed on four different metal substrates. As can be seen, the strongest stresses in silicene occur for the copper substrate and are minimal for the aluminum substrate. However, even in the case of the copper substrate, the maximum local stress σ_{zz}^{max} does not exceed 44% of the ultimate silicene strength upon uniaxial tension.

Designing anodes on the base of defective silicene sheets meets a problem of maintaining the form of these defects during lithiation and delithiation. Fig. 5 shows configurations of upper silicene sheets together with incorporated lithium atoms as a result of intercalation. In general, monovacancies and trivacancies are well maintained on copper and nickel substrates after one cycle. Li atoms often occupy positions at the centers of hexagonal rings formed by Si atoms. Therefore, a partially regular packing of lithium atoms is formed in the channel.

Angular distributions of the nearest geometric neighbors for lithium packings in the channels were obtained using statistical geometry. Fig. 6 shows θ distributions determined for channel walls with bivacancies. Narrow high peaks periodically arranged in region $0 \le \theta \le 180°$ characterize the degree of crystallinity of the packings. The better the resolution of characteristic peaks is, the closer the packing approaches the crystal. As can be seen, the highest and the lowest crystallinity is exhibited lithium packings in the channels on silver and copper substrates, respectively.

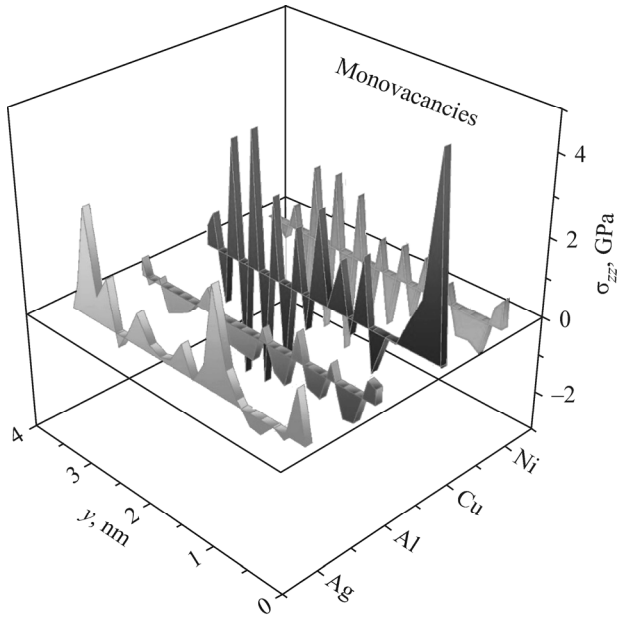

Fig. 4. Distribution of average stresses σ_{zz} in silicene sheets with monovacancies along the 0y (*"chair"*) direction when lithium is intercalated into silicene channels placed on Ag, Al, Cu, and Ni substrates. Surface elements are extended along the 0x axis.

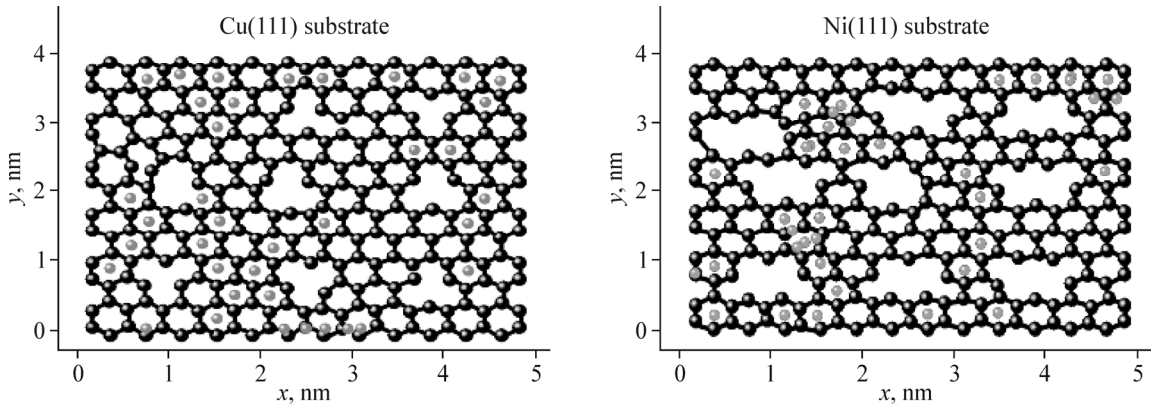

Fig. 5. *xy* projections of the upper silicene layer with mono- and trivacancies on Cu (111) (*a*) and Ni (111) (*b*) substrates after complete lithiation.

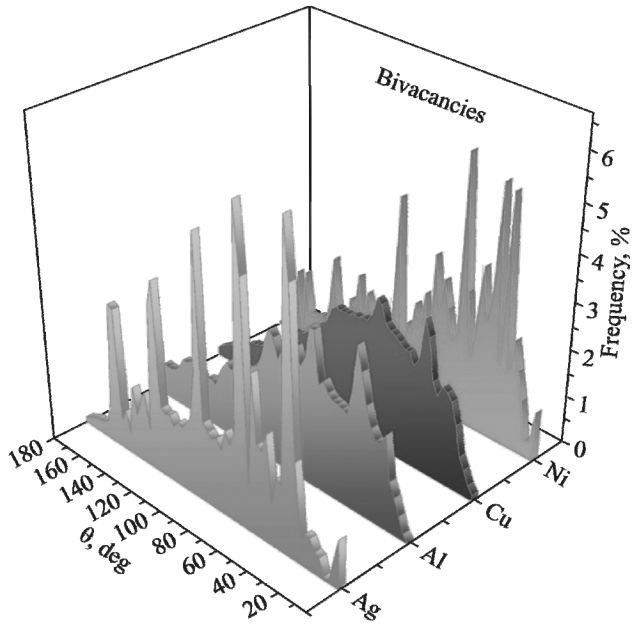

Fig. 6. Angular distributions of the nearest geometric neighbors in lithium packings for silicene channels on Ag, Al, Cu, and Ni substrates. The channel walls contain bivacancies.

Fig. 7 shows the calculated voltage profile $V(x)$ generated by the silicene element. The regions of low Li concentrations demonstrate a small voltage oscillation of ~ 0.75 V. This means that no single stable phase Li_xSi_y exists up to the concentration $x = 1$, which may be related to large number of different sites available on silicene for the deposition of Li atoms. At $x = 1$, the potential becomes negative. Such behavior of $V(x)$ means that adsorption mechanism has been changed, probably, due to the formation of Li–Li bonds and a growing tendency of Si–Si bond breaking. A sharp drop of $V(x)$ can be also explained by the formation of a "phase" with a higher Li content ($x \geq 1$). A stepwise smoothing of $V(x)$ dependence is associated with the formation of characteristic crystalline phases ($Li_{12}Si_7$, Li_7Si_3, $Li_{13}Si_4$ and $Li_{22}Si_5$) if intercalation in silicene carried out at a higher temperature (688 K) [30].

The point on the graph corresponding to $x = 1.45$ shows the beginning of silicene destruction. Since x is as high as 4.4 in the presence of chemical bonding in the "non-destructive" alloy Li_xSi, the charge capacity of a free-standing bilayer silicene filled by lithium can be estimated to be 1384 Ah/g. This value is 13.6% higher than that obtained for monolayer silicene [28].

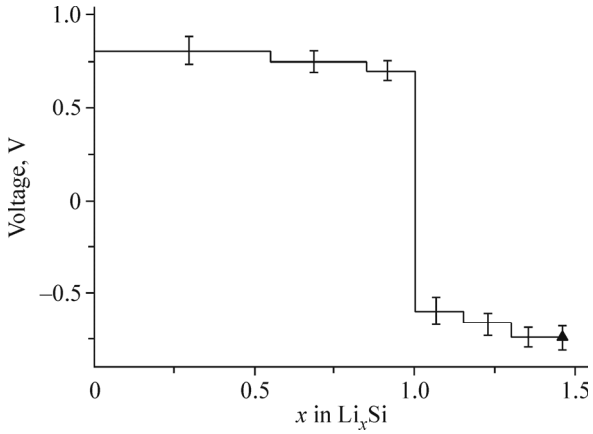

Fig. 7. Calculated voltage profile as a function of the concentration of Li adsorbed on silicene. Vertical line segments show the error of voltage determination. The point on the graph represents a concentration $x = 1.45$ marking the beginning of silicene destruction.

The Tersoff interatomic potential provides a good description of voluminous and elastic properties of silicon. However, it tends to overestimate the lattice barrier to brittle fracture, resulting in an overestimate of the system's viscosity upon destruction [31]. The Morse potentials used in our work imply that the elasticity moduli are fitted to their experimental values for the corresponding crystal. The model does not take into account the formation of the Si–Li alloy due to the formation of chemical bonds. A more accurate description of Si–Li interactions could be achieved by ab initio calculations; however, it would be highly problematic to perform the whole set of above calculations using computationally expensive ab initio molecular dynamics.

CONCLUSIONS

The processes of lithium intercalation and deintercalation into silicene channels on four different metal substrates, including the channels whose walls contain defects, were studied. The highest occupancy by lithium was demonstrated by channels on nickel and copper substrates with defects in the form of mono- and bivacancies, respectively. The self-diffusion coefficient of lithium is a significantly fluctuating function of the channel's occupancy by this metal. The nature of these fluctuations is largely determined by the type of defects in silicene sheets. The stresses normal to the channel walls play an essential role in filling the channel with lithium. In the “chair” direction of atomic rows, the highest and the lowest local stresses appear in the channels on copper and aluminum substrates, respectively. A large part of lithium atoms intercalated into the channel occur above the centers of hexagonal rings formed by Si atoms. As a result, lithium packings acquire a certain degree of crystallinity manifested as periodic narrow peaks of the angular distribution of nearest geometric neighbors. The maximal and minimal crystallinity degrees of lithium packings in the channel are exhibited by the θ spectra of the channels on silver and copper substrates, respectively. The charge capacity of a free-standing bilayer silicene upon intercalation by lithium is estimated to be as high as 1384 mAh/g.

Thus, the performed study shows that silicene may be a promising material for designing anodes of new-generation lithium-ion batteries. The highest lithium occupancy is achieved by using defective silicene channels on Ni(111) and Cu(111) substrates.

FUNDING

This work was financially supported by the Russian Science Foundation (project No. 16-13-00061).

CONFLICT OF INTERESTS

The authors declare that they have no conflict of interests.

REFERENCES

1. H. Sahaf, L. Masson, C. Le′andri, B. Aufray, G. Le Lay, and F. Ronci. *Appl. Phys. Lett.*, **2007**, *90*, 263110.
2. A. Fleurence, R. Friedlein, T. Ozaki, H. Kawai, Y. Wang, and Y. Yamada-Takamura. *Phys. Rev. Lett.*, **2012**, *108*, 245501.
3. L. Meng, Y. Wang, L. Zhang, S. Du, R. Wu, L. Li, Y. Zhang, G. Li, H. Zhou, W. A. Hofer, and H.-J. Gao. *Nano Lett.*, **2013**, *13*, 685.
4. T. Aizawa, S. Suehara, and S. Otani. *J. Phys. Chem. C*, **2014**, *118*, 23049.
5. P. De Padova, C. Quaresima, P. Perfetti, B. Olivieri, B. Le′andri, B. Aufray, S. Vizzini, and G. Le Lay. *Nano Lett.*, **2008**, *8*, 271.
6. S. S. Cahangirov, M. Topsakal, E. Aktürk, H. S′ahin, and S. Ciraci. *Phys. Rev. Lett.*, **2009**, *102*, 236804.
7. A. Y. Galashev and K. A. Ivanichkina. *J. Electrochem. Soc.*, **2018**, *165*, A1788.
8. Y.-S. Choi, J.-H. Park, J.-P. Ahn, and J.-C. Lee. *Sci. Rep.*, **2017**, *7*, 14028.
9. M. Pharr, K. Zhao, X. Wang, Z. Suo, and J. J. Vlassak. *Nano Lett.*, **2012**, *12*, 5039.
10. K. Persson, V. A. Sethuraman, L. J. Hardwick, Y. Hinuma, Y. S. Meng, A. van der Ven, V Srinivasan, R. Kostecki, and G. Ceder. *J. Phys. Chem. Lett.*, **2010**, *1*(8), 1176.
11. A. Y. Galashev and K. A. Ivanichkina. *ChemElectroChem*, **2019**, *6*(5), 1525.
12. A. Y. Galashev, O. R. Rakhmanova, and K. A. Ivanichkina, *J. Struct. Chem.*, **2018**, *59*(4), 877.
13. A. Y. Galashev and K. A. Ivanichkina. *Phys. Lett. A*, **2017**, *381*, 3079.
14. A. Y. Galashev and K. A. Ivanichkina. *Phys. Chem. Chem. Phys.*, **2019**, ***21*,** 12310.
15. J. Tersoff. *Phys. Rev. B: Condens. Matter Mater. Phys.*, **1989**, *39*, 5566.
16. S. M. Foiles, M. I. Baskes, and M. S. Daw. *Phys. Rev. B*, **1986**, *33*, 7983.
17. R. Yu, P. Zhai, G. Li, and L. Liu. *J. Electron. Mater.*, **2012**, *41*, 1465.
18. K.-N. Chiang, C.-Y. Chou, C.-J. Wu, C.-J. Huang, and M.-C. Yew. *ICCES*, **2009**, *9*, 130.
19. S. K. Das, D. Roy, and S. Sengupta. *J. Phys. F: Met. Phys.*, **1977**, *7*, 5.
20. A. Y. Galashev. *Comp. Mater. Sci.*, **2015**, *98*, 123.
21. A. E. Galashev, Yu. P. Zaykov, and R. G. Vladykin. *Russ. J. Electrochemistry*, **2016**, *52*(10), 966.
22. A. E. Galashev, K. A. Ivanichkina, A. S. Vorobiev, and O. R. Rakhmanova. *Phys. Solid State*, **2017**, *59*(6), 1242.
23. P. Ordejon, E. Artacho, and J. M. Soler. *Phys. Rev. B*, **1996**, *53*, 10441.
24. P. Hohenberg and W. Kohn. *Phys. Rev. B*, **1964**, *136*, 864.
25. P. E. Bloechl. *Phys. Rev. B: Condens. Matter Mater. Phys.*, **1994**, *50*, 17953.
26. J. P. Perdew, K. Burke, and M. Ernzerhof. *Phys. Rev. Lett.*, **1996**, *77*, 3865.
27. A. Y. Galashev and A. S. Vorob′ev. *J. Solid State Electrochem.*, **2018**, *22*, 3383.
28. S. Xu, X. Fan, J. Liu, D.J. Singh, Q. Jiang, and W. Zheng. *Phys. Chem. Chem. Phys.*, **2018**, ***20***, 8887.
29. S. Plimpton. *J. Comput. Phys.*, **1995**, *117*, 1.
30. V. Chevrier and J. Dahn. *J. Electrochem. Soc.*, **2009**, *156*, A454.
31. A. P. Bartok, J. Kermode, N. Bernstain, and G. Csanyi. *Phys. Rev. X*, **2018**, *8*(4), 041048.